




# Photosensitivity of Ga<sub>2</sub>O<sub>3</sub> Schottky diodes: Effects of deep acceptor traps present before and after neutron irradiation

Cite as: APL Mater. 8, 111105 (2020); <https://doi.org/10.1063/5.0030105>

Submitted: 21 September 2020 . Accepted: 28 October 2020 . Published Online: 05 November 2020

 E. B. Yakimov, A. Y. Polyakov, I. V. Shchemerov,  N. B. Smirnov, A. A. Vasilev,  P. S. Vergeles, E. E. Yakimov,  A. V. Chernykh, A. S. Shikoh,  F. Ren, and  S. J. Pearton



View Online



Export Citation



CrossMark

## ARTICLES YOU MAY BE INTERESTED IN

[A review of Ga<sub>2</sub>O<sub>3</sub> materials, processing, and devices](#)

Applied Physics Reviews 5, 011301 (2018); <https://doi.org/10.1063/1.5006941>

[Recent progress on the electronic structure, defect, and doping properties of Ga<sub>2</sub>O<sub>3</sub>](#)

APL Materials 8, 020906 (2020); <https://doi.org/10.1063/1.5142999>

[Influence of growth temperature on defect states throughout the bandgap of MOCVD-grown β-Ga<sub>2</sub>O<sub>3</sub>](#)

Applied Physics Letters 117, 172106 (2020); <https://doi.org/10.1063/5.0025970>

**AVS Quantum Science**  
Now Publishing Original Research

Co-Published by



LEARN MORE



# Photosensitivity of Ga<sub>2</sub>O<sub>3</sub> Schottky diodes: Effects of deep acceptor traps present before and after neutron irradiation

Cite as: APL Mater. 8, 111105 (2020); doi: 10.1063/5.0030105  
Submitted: 21 September 2020 • Accepted: 28 October 2020 •  
Published Online: 5 November 2020



E. B. Yakimov,<sup>1,2</sup> A. Y. Polyakov,<sup>2</sup> I. V. Shchemerov,<sup>2</sup> N. B. Smirnov,<sup>2</sup> A. A. Vasilev,<sup>2</sup> P. S. Vergeles,<sup>1</sup> E. E. Yakimov,<sup>1</sup> A. V. Chernykh,<sup>2</sup> A. S. Shikoh,<sup>2</sup> F. Ren,<sup>3</sup> and S. J. Pearton<sup>4,a)</sup>

## AFFILIATIONS

<sup>1</sup>Institute of Microelectronics Technology and High Purity Materials, Russian Academy of Sciences, Moscow 142432, Russia

<sup>2</sup>National University of Science and Technology MISiS, Moscow 119049, Russia

<sup>3</sup>Department of Chemical Engineering, University of Florida, Gainesville, Florida 32611, USA

<sup>4</sup>Department of Materials Science and Engineering, University of Florida, Gainesville, Florida 32611, USA

<sup>a)</sup> Author to whom correspondence should be addressed: [spear@mse.ufl.edu](mailto:spear@mse.ufl.edu)

## ABSTRACT

The photocurrent produced by 259 nm wavelength excitation was measured in  $\beta$ -Ga<sub>2</sub>O<sub>3</sub> Schottky diodes before and after neutron irradiation. These samples differed by the density of deep acceptors in the lower half of the bandgap as detected by capacitance–voltage profiling under monochromatic illumination. Irradiation led to a very strong increase in photocurrent, which closely correlated with the increase in deep trap density and the decrease after illumination of the effective Schottky barrier height due to hole capture by acceptors. A similar effect was observed on an as-grown  $\beta$ -Ga<sub>2</sub>O<sub>3</sub> film with a high density of deep acceptors. Electron beam induced current measurements indicated a strong amplification of photocurrent, which is attributed to the Schottky barrier lowering by holes trapped on acceptors near the surface. Photocurrent build-up and decay curves show several time constants ranging from several milliseconds to many seconds. These characteristic times are attributed to tunneling of electrons into the hole-filled acceptors near the surface and to thermal emission of holes from deep acceptors.

© 2020 Author(s). All article content, except where otherwise noted, is licensed under a Creative Commons Attribution (CC BY) license (<http://creativecommons.org/licenses/by/4.0/>). <https://doi.org/10.1063/5.0030105>

The transparent wide-bandgap semiconductor Ga<sub>2</sub>O<sub>3</sub> has excellent potential for applications in power electronics<sup>1,2</sup> and solar-blind photodetectors.<sup>2–4</sup> In the latter case, the advantage is due to the bandgap close to 5 eV, rendering photodetectors based on Ga<sub>2</sub>O<sub>3</sub> to be only sensitive to photons in the far-UV spectral range and also to exhibit a high photosensitivity. There have been many recent reports on photoresponse properties of Ga<sub>2</sub>O<sub>3</sub> photodetectors, both for the interdigital back-to-back Schottky diode architecture operation at high applied voltages and for simple Schottky diode architectures in both photovoltaic and biased modes.<sup>3–12</sup> Many of these report an extremely high external quantum efficiency (EQE) of photoresponse, often exceeding hundreds or even thousands in percentage.<sup>3–12</sup> To explain such high EQE values in Ga<sub>2</sub>O<sub>3</sub>-based Schottky diodes, impact ionization amplification<sup>5,6,8</sup> and

modulation of the Schottky barrier height by self-trapped polaronic hole states (STH)<sup>7</sup> or by hole accumulation near the Schottky metal<sup>3</sup> have been proposed.

However, the electric field strength in all reported experiments is far short of the impact ionization threshold of around 5 MV/cm–8 MV/cm<sup>1,2,13</sup> estimated for  $\beta$ -Ga<sub>2</sub>O<sub>3</sub>. As for STH-related charge accumulation in Ga<sub>2</sub>O<sub>3</sub> Schottky diodes, it has been shown recently that above ~140 K and certainly at room temperature, mobile holes rather than STH polaronic states are dominant and mainly contribute to the formation of photocurrent or electron beam induced current (EBIC).<sup>14–17</sup> At the same time, it is well known that a variety of deep hole traps in the lower half of the bandgap can be formed in Ga<sub>2</sub>O<sub>3</sub> and give rise to significant hole trapping in the space charge region<sup>18</sup> with potentially a similar effect on the Schottky

barrier height and photocurrent EQE as the STH states proposed in Ref. 7. In a recent paper on the EBIC collection efficiency in  $\beta$ -Ga<sub>2</sub>O<sub>3</sub>,<sup>17</sup> it was reported that an increased hole trap concentration favored a better collection efficiency. One would expect that similar beneficial effects should be observed for photocurrent and possibly lead to a high photocurrent EQE. To check this assumption, we performed photocurrent and EBIC measurements on  $\beta$ -Ga<sub>2</sub>O<sub>3</sub> Schottky diodes vastly differing in their density of deep hole traps. These experiments convincingly show that the photosensitivity of  $\beta$ -Ga<sub>2</sub>O<sub>3</sub> Schottky diode detectors increases with the increase in density of deep hole traps in the lower half of the bandgap. This helps suggest how the photosensitivity of such detectors can be improved.

The samples studied in this work were acquired from Tamura/Novel Crystals Technology (Japan). They were grown by halide vapor phase epitaxy (HVPE) on bulk substrates grown by Edge-defined Film-fed Growth (EFG). The orientation of the substrates according to the manufacturer's specification was (010). The HVPE films were doped with Si, with starting shallow donor concentration for one sample  $1.3 \times 10^{16} \text{ cm}^{-3}$  and  $1.1 \times 10^{17} \text{ cm}^{-3}$  for the other. The substrates were doped with Sn to a net donor concentration of  $3 \times 10^{18} \text{ cm}^{-3}$ . The thickness of the HVPE films was 10  $\mu\text{m}$ , and the substrate thickness was 650  $\mu\text{m}$ . For the lower doped HVPE film, three pieces were studied: one before neutron irradiation (henceforth called sample 1) and two after neutron irradiation with fast neutron fluences of  $5 \times 10^{13} \text{ cm}^{-2}$  (sample 1\_5E13) and  $4 \times 10^{14} \text{ cm}^{-2}$  (sample 1\_4E14), respectively. Irradiation was done using a two-zone pulsed self-extinguishing fast-neutron reactor BARS-6.<sup>19</sup> For these three samples, net donor concentrations from capacitance-voltage (C-V) profiling, deep electron trap spectra from deep level transient spectroscopy (DLTS),<sup>20</sup> and deep hole trap spectra from C-V profiling under monochromatic light illumination (LCV)<sup>21,22</sup> were measured.<sup>19</sup> The net donor concentration decreased from  $1.3 \times 10^{16} \text{ cm}^{-3}$  in the virgin sample 1 to  $5.3 \times 10^{15} \text{ cm}^{-3}$  in sample 1\_4E14. In deep electron trap spectra, the E2 traps near  $E_c - 0.8 \text{ eV}$  related to Fe acceptors<sup>23–25</sup> and native-defects-related E2\* ( $E_c - 0.75 \text{ eV}$ ), E3 ( $E_c - 1 \text{ eV}$ ), and E4 ( $E_c - 1.2 \text{ eV}$ )<sup>26</sup> traps were detected. The concentration of the dominant E2 traps was  $2 \times 10^{14} \text{ cm}^{-3}$  for all samples, while the concentrations of other traps increased with neutron fluence from low  $10^{13} \text{ cm}^{-3}$  in sample 1 to  $1.5 \times 10^{14} \text{ cm}^{-3}$  in sample 1\_4E14.<sup>19</sup> The main deep acceptor traps detected in LCV spectra had optical ionization thresholds close to 2.3 eV and 3.1 eV, both associated in the literature with Ga vacancy acceptor related defects.<sup>19</sup>

The properties of traps in the S2 sample have been reported elsewhere.<sup>17</sup> The concentration profile of this sample calculated from C-V data, the spectral dependence of photoconcentration  $\Delta N_{ph}$  obtained from LCV data, electron traps DLTS spectra for this sample are shown in Figs. 1S–3S of the [supplementary material](#). In sample S2, the dominant electron trap is the E2 Fe-related center with a concentration of  $7 \times 10^{15} \text{ cm}^{-3}$  and a lower concentration of  $1.5 \times 10^{15} \text{ cm}^{-3}$  in E3 traps. The types of deep acceptor traps in LCV spectra were similar to those in sample 1, but the concentrations were about an order of magnitude higher. For the subject of this paper, the variations in the density of deep hole traps are of most importance. Respective values are presented in Table I.

For all samples, transparent front surface Ni Schottky diodes with a diameter of 1.2 mm and a metal thickness of 20 nm were

**TABLE I.** Net donor concentrations  $N_d$ , concentrations of deep hole traps with an optical ionization energy of 2.3 eV [N (2.3 eV)], traps with an optical ionization energy of 3.1 eV [N (3.1 eV)], and the persistent change in the Schottky barrier height  $\Delta V_{bi}$  in C-V characteristics after illumination with 259 nm LED.

Sample no.	$N_d$ ( $\times 10^{16} \text{ cm}^{-3}$ )	N (2.3 eV) ( $\times 10^{14} \text{ cm}^{-3}$ )	N (3.1 eV) ( $\times 10^{14} \text{ cm}^{-3}$ )	$\Delta V_{bi}$ (V)
S1	1.4	2	...	0.03
S1_5E13	1.2	3	1.1	0.09
S1_5E14	0.53	7.7	2.7	0.15
S2	11	20	20	0.35

prepared by electron beam evaporation through a shadow mask. The back Ohmic contacts were made by Ti/Au electron beam evaporation on the substrate side surface preliminarily subjected to Ar plasma treatment and subsequent rapid thermal annealing at 300 °C.<sup>27</sup> For neutron irradiation, the Ohmic contacts were prepared before irradiation, while the Schottky diodes were deposited after irradiation. Current-voltage (I-V) characteristics were measured in the dark and under illumination using two-channel B2902A voltage/current source/meter (Keysight Technologies, USA). For illumination, GaN-based light emitting diodes with a peak wavelength of 259 nm (QPhotonics LLC, USA) were used. Three LEDs were bunched together and connected in series to produce a light spot of 5 mm in diameter with maximum optical output density within this 5 mm spot of  $5 \times 10^{-4} \text{ W/cm}^2$ . Dark I-V measurements were performed at different temperatures from 100 K to 460 K to determine the ideality factor and saturation current in the forward direction and estimate the Schottky barrier height. C-V measurements in the dark, under 259 nm illumination, and after illumination were performed using the E4980A LCR meter (KeySight Technologies, USA, frequency range 20 Hz to 1 MHz).

The EBIC measurements were carried out at 300 K in a scanning electron microscope JSM-840A (JEOL, Japan) using a Keithley 428 current amplifier to measure the beam current  $I_b$  and the EBIC current  $I_c$  at the beam energy  $E_b$ . In these experiments, the value of EBIC current  $I_c$  normalized by the product of the beam energy  $E_b$  and the beam current  $I_b$ ,  $I_c/(I_b \times E_b)$  was measured as a function of the bias applied to the Schottky diode and of beam energy. This was then compared to theoretical predictions based on calculating the beam penetration depth and the spatial distribution of the electron-hole generation function.<sup>15,17</sup> After switching off the excitation, the dark current was larger than that before excitation and slowly decayed to the initial value. To minimize this effect, the Schottky barrier was irradiated with an e-beam pulse of 1.5 s duration and small beam currents, with values chosen to obtain a measurable induced current.

We also monitored the kinetics of photocurrent buildup and decay with step-wise illumination with the 259 nm LED. The photocurrent transients were measured using the B2902A meter, with a time step of 0.2 ms up to times of 30 s–60 s. The measurements were performed from 300 K to 400 K, with the temperature stabilized with an accuracy better than 0.1 K. Figure 4S of the [supplementary material](#) also shows the room temperature micro-cathodoluminescence (MCL) spectra of the samples.

Dark I–V characteristics of all samples showed good ideality in the forward direction, with the ideality factor close to 1 and saturation current in the forward direction showing an activation energy of 1.05 eV–1.1 eV, corresponding to the Schottky barrier height (actual data presented in the [supplementary material](#)). In the reverse direction, the current showed a measurable dependence on voltage and a slight temperature dependence with an effective activation energy of  $\sim 0.3$  eV, suggesting tunneling assisted current flow involving traps. The 300 K reverse I–V characteristics in the dark and with 259 nm LED illumination are shown for samples S1, S1\_5E13, and S1\_5E14 in [Fig. 1](#). The photocurrent markedly increases with the neutron irradiation dose and applied voltage. For a reverse voltage of  $-60$  V, the photocurrent increased by 2.5 times after irradiation with  $5 \times 10^{13}$  cm $^{-2}$  neutrons and by 18 times for  $4 \times 10^{14}$  cm $^{-2}$  neutrons compared with the virgin sample S1. For sample S2, the photocurrent measurements could only be done up to  $-40$  V, but at this lower voltage, the photocurrent density was 0.02 A/cm $^2$ , i.e., almost 1000 times higher than that for sample S1 (data can be found in the [supplementary material](#)).

The EBIC collection efficiency dependence on applied voltage for samples S1, S2, and S1\_4E14 is shown in [Fig. 2](#). The measurements were done with a beam electron energy of 4 kV, which generates charge carriers down to a depth of 50 nm from the surface, i.e., well within the space charge region of the Schottky diode.<sup>17</sup> Under these conditions, normally, the entire charge of the generated electron–hole pairs should be fully collected and the calculated normalized value of the EBIC signal  $I_c/(I_b \times E_b)$  should be close to 15 keV $^{-1}$  and should not depend on voltage until the onset of the charge multiplication caused by the band-to-band impact ionization or the impact ionization of deep traps.<sup>17</sup> This is approximately the case for sample 1 up to a voltage of 150 V, when the signal starts to increase (the voltage corresponds to the maximal electric field in the diode close to  $10^6$  V/cm). After irradiation with  $4 \times 10^{14}$  n/cm $^2$  neutrons, the normalized EBIC signal at high applied voltages is about an order of magnitude higher than expected, while for the S2 sample, the actual signal is orders of magnitude higher than predicted.

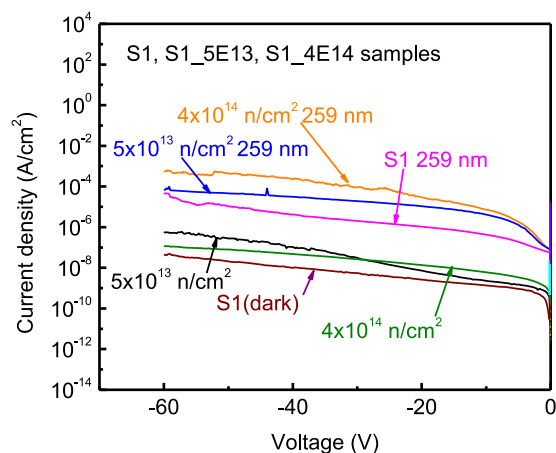


**FIG. 1.** Room temperature dark reverse current and photocurrent under 259 nm LED illumination for three samples of  $\beta$ -Ga $_2$ O $_3$  Schottky diodes.

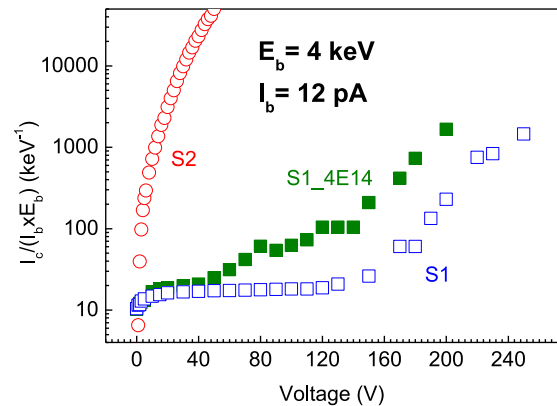


**FIG. 2.** Normalized EBIC signal as a function of applied reverse bias for samples S1, S2, and S1\_4E14 with the probing beam electrons energy of 4 keV and the beam current of 12 pA.

This discrepancy suggests the existence of a multiplication mechanism. The bulk impact ionization can be excluded because the electric field strength for which amplification is observed in our samples does not exceed  $10^6$  V/cm, i.e., far short of predicted values of 5 MV/cm–8 MV/cm.<sup>2,13</sup> Another option is the photocurrent amplification driven by lowering of the Schottky barrier height by the excessive charge localized near the metal interface.<sup>7</sup> In [Ref. 7](#), it was proposed that the phenomenon is related to polaronic self-trapped holes, but positive charge accumulation on deep acceptor states should lead to a similar effect. In [Fig. 3](#), we show the charge concentration profiles deduced for samples S1, S1\_5E13, and S1\_4E14 from C–V profiling in the dark and under 259 nm LED illumination. A considerable increase in the charge concentration occurs down to  $\sim 1$   $\mu$ m from the surface upon illumination. The holes trapped on the deep centers below the Fermi level should change the apparent Schottky barrier height. Solving the Poisson equation yields the decrease in the apparent barrier height as  $\Delta V_{bi} = N_{deep} \times q \times w_o^2 / (2\epsilon\epsilon_o)$ ,<sup>28</sup> where  $N_{deep}$  is the density of deep traps that have been recharged,  $w_o$  is the depth to which the traps have been recharged

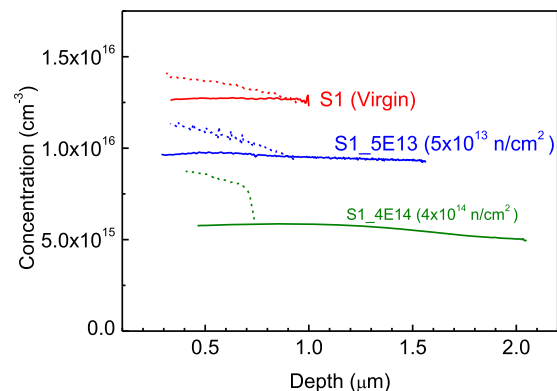


**FIG. 3.** Dark (solid line) charge concentration profiles and profiles measured with 259 nm illumination (dashed line) for three  $\beta$ -Ga $_2$ O $_3$  Schottky diode samples S1, S1\_5E13, and S1\_4E14.

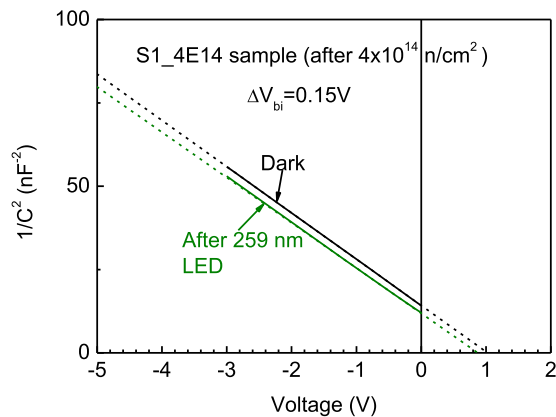


**FIG. 4.** Room temperature  $1/C^2$  vs  $V$  plots measured in the dark and after illumination with the 259 nm LED for sample S1\_4E14.

during illumination,  $q$  is the electronic charge,  $\epsilon_0$  is the dielectric constant of vacuum, and  $\epsilon$  is the relative dielectric constant.

The effect manifests itself in the decrease in the voltage offset in the  $1/C^2$  vs  $V$  plots measured in the dark and after illumination by  $\Delta V_{bi}$ .<sup>28</sup> Figure 4 shows such  $C$ - $V$  plots measured at 300 K before and after illumination with the 259 nm LED for sample S1\_4E14. Before illumination, the voltage offset is 1.03 V giving a barrier height close to that obtained from  $I$ - $V$  measurements. After illumination, the voltage offset decreased by 0.15 V because of the charge of holes trapped on deep acceptors. The density of charge trapped on deep acceptors estimated from this  $\Delta V_{bi}$  shift is  $\sim 8 \times 10^{14} \text{ cm}^{-3}$  and is similar to the density of deep hole traps determined from LCV profiling in Ref. 19 and presented in Table I. For other samples, the changes in the barrier height caused by trapping during illumination are presented in Table I. In a simple approach, these changes in the barrier height should convert themselves into the exponential increase in the current flowing through the Schottky diode. Figure 5 shows this increase in current for samples S1, S1\_5E13, and S1\_4E14

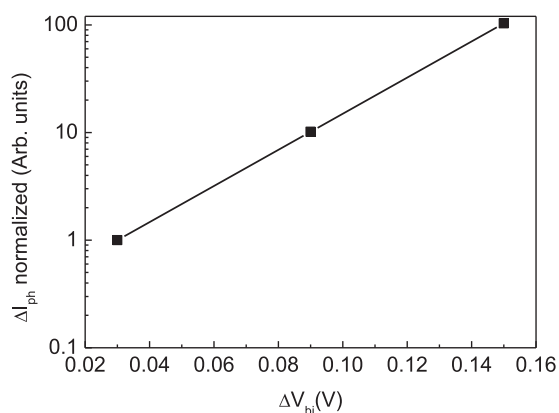


**FIG. 5.** Changes expected in photocurrent for the Schottky barrier height of 1 eV assuming that the changes are caused by the change in the Schottky barrier height produced by charging the deep acceptor traps; the points correspond to the changes in  $\Delta V_{bi}$  observed in samples S1, S1\_5E13, and S1\_4E14 after 259 nm LED illumination.

(the results are normalized to the value for sample S1). The amount of increase in the samples photocurrent is qualitatively similar to the actual changes in photocurrent with increased density of deep acceptor traps and at least, in part, explains the observed multiplication of the signal in photocurrent measurements.

There is, however, a problem related to the proposed mechanism in terms of the disposal of the charge accumulated on deep acceptors. The depth of the centers is quite high and thermal emission of holes captured during illumination should be very slow at room temperature and strongly depends on the temperature. The actual times of photocurrent buildup and decay in  $\text{Ga}_2\text{O}_3$  photodetectors<sup>3</sup> are indeed quite long, many seconds to minutes. However, the waveform of the transient photocurrent and the effects of temperature on characteristic times are generally not reported.

The results of actual measurements performed for the S1 and S1\_4E14 samples of the present set (Fig. 6 shows the data for sample 1\_4E14, in the [supplementary material](#), we present the same data on a shorter time scale and similar data for sample 1) show that (a) the build-up and decay times are indeed very long, many seconds, and (b) the photocurrent transients cannot be represented as single exponents, but consist of several exponential decays for which the shortest decay time is close to 100 ms and very weakly depends on temperature, while for longer times, several other decay processes take place with much longer time constants that become shorter with increased temperature. These longer decay times could be related to deep hole traps emitting holes thermally, while the short decay time weakly dependent on temperature could be due to electrons tunneling from the metal contact into the deep trap states filled with holes.

While a more detailed understanding of the mechanisms involved is needed, our current model summarized by Fig. 7 is as follows: Electrons and holes are produced in the space charge region by illumination and holes slowly drift to the metal contact and, on the way, are captured by deep hole traps, thus varying the built-in charge and lowering the Schottky barrier height, the main cause of high gain in photocurrent. The photocurrent decay occurs by tunneling of electrons from the metal into the acceptor states filled with holes near the metal and by thermal emission of holes deeper in the material. The hole trap states closest to the surface should be most

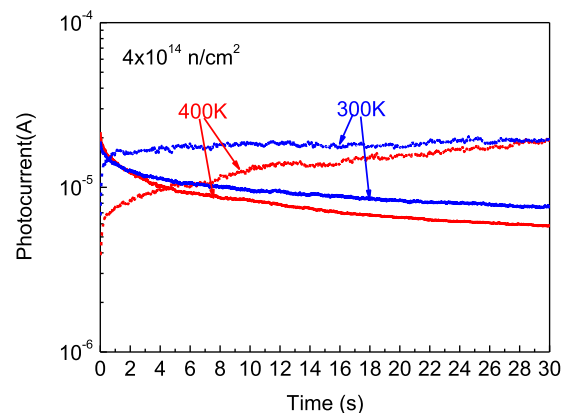


**FIG. 6.** Photocurrent build-up and decay curves for 300 K and 400 K for sample S1\_4E14.

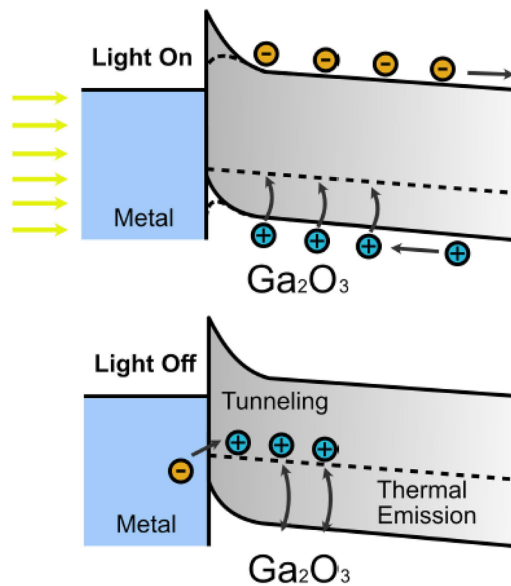


**FIG. 7.** Schematic representation of the processes involved in photocurrent build-up and decay in  $\beta$ -Ga<sub>2</sub>O<sub>3</sub> Schottky diodes.

significant in varying the Schottky barrier height. This explains the marked dependence of the photocurrent on applied voltage, since holes in Ga<sub>2</sub>O<sub>3</sub> are heavy and a high electric field is necessary to accelerate them and efficiently deliver them close to the surface.

In summary, the photocurrent in  $\beta$ -Ga<sub>2</sub>O<sub>3</sub> Schottky diodes can be strongly enhanced when the density of deep hole traps in the lower half of the bandgap is increased. The effect is attributed to the accumulation of holes on these acceptors giving rise to the increased space charge density near the surface leading to a decrease in the Schottky barrier height and corresponding photocurrent amplification. The efficiency of the process is boosted by increasing the electric field in the space charge region to increase the hole velocity and facilitates their delivery to the near-surface region where the local charge buildup is most conducive to the decrease in the Schottky barrier height. The photocurrent decay is provided by electrons tunneling into the deep acceptor states filled with holes near the surface and by thermal emission of holes from deep acceptors that are further removed from the surface. This explains the unusually long photocurrent build-up and decay times commonly observed in  $\beta$ -Ga<sub>2</sub>O<sub>3</sub> Schottky diodes.<sup>3</sup> This peculiar mechanism of photocurrent flow in  $\beta$ -Ga<sub>2</sub>O<sub>3</sub> Schottky diodes explains the unexpected increase in photocurrent of such diodes after irradiation. Understanding this mechanism also suggests approaches to improving the photosensitivity of  $\beta$ -Ga<sub>2</sub>O<sub>3</sub> Schottky diodes. Specifically, since most of the deep acceptors in the lower half of the bandgap are attributed to defects related to Ga vacancy acceptors,<sup>16,26</sup> the photosensitivity is expected to be increased by treatments enhancing the density of Ga vacancies: growth under O-rich conditions, high-energy particle irradiations that increase the density of Ga vacancies,<sup>19,26</sup> surface treatment in ozone (reported to be beneficial for photosensitivity<sup>3</sup>), and high-energy plasma treatment shown to generate defects in the lower half of the bandgap of gallium oxide.<sup>29</sup>

See the [supplementary material](#) for the detailed material properties of the Ga<sub>2</sub>O<sub>3</sub> structures used in these experiments.

The work at the NUST MISiS was supported, in part, by Grant No. K2-2020-011 under the Program to increase Competitiveness of NUST MISiS among the World Leading Scientific and Educational centers (Program funded by the Russian Ministry of Science and Education). The work at IMT RAS was supported, in part, by State Task No. 075-00920-20-00. The work at UF was sponsored by the Department of the Defense, Defense Threat Reduction Agency (Grant No. HDTRA1-17-1-011), monitored by J. Calkins, DTRA Interaction of Ionizing Radiation with Matter University Research Alliance (Grant No. HDTRA1-19-S-0004; Jacob Calkins) and also by the NSF DMR (Grant No. 1856662; James Edgar).

## DATA AVAILABILITY

The data that support the findings of this study are available within the article and its [supplementary material](#).

## REFERENCES

- S. J. Pearton, F. Ren, M. Tadjer, and J. Kim, "Perspective: Ga<sub>2</sub>O<sub>3</sub> for ultra-high power rectifiers and MOSFETS," *J. Appl. Phys.* **124**, 220901 (2018).
- S. J. Pearton, J. Yang, P. H. Cary, F. Ren, J. Kim, M. J. Tadjer, and M. A. Mastro, "A review of Ga<sub>2</sub>O<sub>3</sub> materials, processing and devices," *Appl. Phys. Rev.* **5**, 011301 (2018).
- J. Xu, W. Zheng, and F. Huang, "Gallium oxide solar-blind ultraviolet photodetectors: A review," *J. Mater. Chem. C* **7**, 8753 (2019).
- X. Chen, F. Ren, S. Gu, and J. Ye, "Review of gallium-oxide-based solar-blind ultraviolet photodetectors," *Photonics Res.* **7**, 381–415 (2019).
- G. C. Hu, C. X. Shan, N. Zhang, M. M. Jiang, S. P. Wang, and D. Z. Shen, "High gain Ga<sub>2</sub>O<sub>3</sub> solar-blind photodetectors realized via a carrier multiplication process," *Opt. Express* **23**, 13554 (2015).
- B. Qiao, Z. Zhang, X. Xie, B. Li, K. Li, X. Chen, H. Zhao, K. Liu, L. Liu, and D. Shen, "Avalanche gain in metal-semiconductor-metal Ga<sub>2</sub>O<sub>3</sub> solar-blind photodiodes," *J. Phys. Chem. C* **123**, 18516 (2019).
- A. M. Armstrong, M. H. Crawford, A. Jayawardena, A. Ahyi, and S. Dhar, "Role of self-trapped holes in the photoconductive gain of  $\beta$ -Ga<sub>2</sub>O<sub>3</sub> Schottky diodes," *Appl. Phys.* **119**, 103102 (2016).
- S. Oh, H. W. Kim, and J. Kim, "High gain  $\beta$ -Ga<sub>2</sub>O<sub>3</sub> solar-blind Schottky barrier photodiodes via carrier multiplication process," *ECS J. Solid State Sci. Technol.* **7**, Q196 (2018).
- Y. Qin, L. Li, X. Zhao, G. S. Tompa, H. Dong, G. Jian, Q. He, P. Tan, X. Hou, Z. Zhang, S. Yu, H. Sun, G. Xu, X. Miao, K. Xue, S. Long, and M. Liu, "Metal-semiconductor-metal  $\epsilon$ -Ga<sub>2</sub>O<sub>3</sub> solar-blind photodetectors with a record-high responsivity rejection ratio and their gain mechanism," *ACS Photonics* **7**, 812 (2020).
- X. Chen, F.-F. Ren, J. Ye, and S. Gu, "Gallium oxide-based solar-blind ultraviolet photodetectors," *Semicond. Sci. Technol.* **35**, 023001 (2020).
- Z. X. Jiang, Z. Y. Wu, C. C. Ma, J. N. Deng, H. Zhang, Y. Xu, J. D. Ye, Z. L. Fang, G. Q. Zhang, J. Y. Kang, and T.-Y. Zhang, "P-type  $\beta$ -Ga<sub>2</sub>O<sub>3</sub> metal-semiconductor-metal solar-blind photodetectors with extremely high responsivity and gain-bandwidth product," *Mater. Today Phys.* **14**, 100226 (2020).
- H. Kim, S. Tarelkin, A. Polyakov, S. Troschiev, S. Nosukhin, M. Kuznetsov, and J. Kim, "Ultrawide-bandgap p-n heterojunction of diamond/ $\beta$ -Ga<sub>2</sub>O<sub>3</sub> for a solar-blind photodiode," *ECS J. Solid State Sci. Technol.* **9**, 045004 (2020).
- K. Ghosh and U. Singiseti, "Impact ionization in  $\beta$ -Ga<sub>2</sub>O<sub>3</sub>," *J. Appl. Phys.* **124**, 085707 (2018).

- <sup>14</sup>A. Y. Polyakov, N. B. Smirnov, I. V. Shchemerov, S. J. Pearton, F. Ren, A. V. Chernykh, P. B. Lagov, and T. V. Kulevoy, "Hole traps and persistent photocapacitance in proton irradiated Ga<sub>2</sub>O<sub>3</sub> films doped with Si," *APL Mater.* **6**, 096102 (2018).
- <sup>15</sup>E. B. Yakimov, A. Y. Polyakov, N. B. Smirnov, I. V. Shchemerov, J. Yang, F. Ren, G. Yang, J. Kim, and S. J. Pearton, "Diffusion length of non-equilibrium minority charge carriers in  $\beta$ -Ga<sub>2</sub>O<sub>3</sub> measured by electron beam induced current," *J. Appl. Phys.* **123**, 185704 (2018).
- <sup>16</sup>E. B. Yakimov and A. Y. Polyakov, "Defects and carrier lifetimes in Ga<sub>2</sub>O<sub>3</sub>," in *Wide Bandgap Semiconductor-Based Electronics*, edited by R. Fan and S. Pearton (IOP Publishers, 2020), Chap. 5.
- <sup>17</sup>E. B. Yakimov, A. Y. Polyakov, N. B. Smirnov, I. V. Shchemerov, P. S. Vergeles, E. E. Yakimov, A. V. Chernykh, M. Xian, F. Ren, and S. J. Pearton, "Role of hole trapping by deep acceptors in electron beam induced current measurements in  $\beta$ -Ga<sub>2</sub>O<sub>3</sub> vertical rectifiers," *J. Phys. D* **53**, 495108 (2020).
- <sup>18</sup>J. Kim, S. J. Pearton, C. Fares, J. Yang, R. Fan, S. Kim, and A. Y. Polyakov, "Radiation damage effects in Ga<sub>2</sub>O<sub>3</sub> materials and devices," *J. Mater. Chem. C* **7**, 10 (2018).
- <sup>19</sup>A. Y. Polyakov, N. B. Smirnov, I. V. Shchemerov, A. A. Vasilev, E. B. Yakimov, A. V. Chernykh, A. I. Kochkova, P. B. Lagov, Y. S. Pavlov, O. F. Kukharchuk, A. A. Suvorov, N. S. Garanin, I.-H. Lee, M. Xian, F. Ren, and S. J. Pearton, "Pulsed fast reactor neutron irradiation effects in Si doped n-type  $\beta$ -Ga<sub>2</sub>O<sub>3</sub>," *J. Phys. D: Appl. Phys.* **53**, 274001 (2020).
- <sup>20</sup>*Capacitance Spectroscopy of Semiconductors*, edited by J. V. Li and G. Ferrari (Pan Stanford Publishing Pte. Ltd., Singapore, 2018), p. 437.
- <sup>21</sup>Z. Zhang, E. Farzana, A. R. Arehart, and S. A. Ringel, "Deep level defects throughout the bandgap of (010)  $\beta$ -Ga<sub>2</sub>O<sub>3</sub> detected by optically and thermally stimulated defect spectroscopy," *Appl. Phys. Lett.* **108**, 052105 (2016).
- <sup>22</sup>E. Farzana, E. Ahmadi, J. S. Speck, A. R. Arehart, and S. A. Ringel, "Deep level defects in Ge-doped (010)  $\beta$ -Ga<sub>2</sub>O<sub>3</sub> layers grown by plasma-assisted molecular beam epitaxy," *J. Appl. Phys.* **123**, 161410 (2018).
- <sup>23</sup>A. T. Neal, S. Mou, S. Rafique, H. Zhao, E. Ahmadi, J. S. Speck, K. T. Stevens, J. D. Blevins, D. B. Thomson, N. Moser, K. D. Chabak, and G. H. Jessen, "Donors and deep acceptors in  $\beta$ -Ga<sub>2</sub>O<sub>3</sub>," *Appl. Phys. Lett.* **113**, 062101 (2018).
- <sup>24</sup>A. Y. Polyakov, N. B. Smirnov, I. V. Shchemerov, S. J. Pearton, F. Ren, A. V. Chernykh, and A. I. Kochkova, "Electrical properties of bulk semi-insulating  $\beta$ -Ga<sub>2</sub>O<sub>3</sub> (Fe)," *Appl. Phys. Lett.* **113**, 142102 (2018).
- <sup>25</sup>M. E. Ingebrigtsen, J. B. Varley, A. Y. Kuznetsov, B. G. Svensson, G. Alfieri, A. Mihaila, U. Badstübner, and L. Vines, "Iron and intrinsic deep level states in Ga<sub>2</sub>O<sub>3</sub>," *Appl. Phys. Lett.* **112**, 042104 (2018).
- <sup>26</sup>A. Y. Polyakov, N. B. Smirnov, I. V. Shchemerov, E. B. Yakimov, S. J. Pearton, C. Fares, J. Yang, F. Ren, J. Kim, P. B. Lagov, V. S. Stolbunov, and A. Kochkova, "Defects responsible for charge carrier removal and correlation with deep level introduction in irradiated  $\beta$ -Ga<sub>2</sub>O<sub>3</sub>," *Appl. Phys. Lett.* **113**, 092102 (2018).
- <sup>27</sup>A. Y. Polyakov, N. B. Smirnov, I. V. Shchemerov, E. B. Yakimov, J. Yang, F. Ren, G. Yang, J. Kim, A. Kuramata, and S. J. Pearton, "Effect of 10 MeV proton irradiation on electrical properties and recombination in Ga<sub>2</sub>O<sub>3</sub> Schottky diodes," *Appl. Phys. Lett.* **112**, 032107 (2018).
- <sup>28</sup>A. Y. Polyakov and I.-H. Lee, "Deep traps in GaN-based structures as affecting the performance of GaN devices (a review)," *Mater. Sci. Eng., R* **94**, 1–56 (2015).
- <sup>29</sup>A. Y. Polyakov, I.-H. Lee, N. B. Smirnov, E. B. Yakimov, I. V. Shchemerov, A. V. Chernykh, A. I. Kochkova, A. A. Vasilev, P. H. Carey, F. Ren, D. J. Smith, and S. J. Pearton, "Defects at the surface of  $\beta$ -Ga<sub>2</sub>O<sub>3</sub> produced by Ar plasma exposure," *APL Mater.* **7**, 061102 (2019).